Monitoring Ecological Crisis of Kolkata Metropolitan Area using Spatial Technology

Pritam Mitra, S.K Mustak* & Prosenjit Barman

Department of Geography, Central University of Punjab, Bathinda, India
*Corresponding Author's email: sk.mustak@cu.edu.in

Abstract

Assessing the quality of urban ecology is indispensable with the dynamic levels of urbanization as this is an important parameter for sustainable development. The rapid population growth with fast urban shift for last three decades is results into eco-health destruction and challenge. This continuous damage calls for quick revitalization of the urban ecosystem. The main objective of this study is to find out ecological crisis including air quality with the help of satellite imagery. The Kolkata Metropolitan Area (KMA) is chosen as study area because it is the rapidly growing densest Indian metropolitan city and listed among world's top air polluted cities. In order to accomplish the study, multidate Landsat 8, Sentinel-2A and Sentinel-5P satellite data from 2018 to 2022 were used. The ecological crisis status was derived in sequential stages as a combination of remote sensing ecological index (RSEI) and air pollution index (API) named as air quality remote sensing ecological index (AQRSEI). First, among the four different indicators of RSEI, greenness, dryness and wetness were measured based on Sentinel-2A satellite data and temperature was measured based on Landsat 8 satellite data. Second, NO2, SO2, O3, and CO were measured based on Sentinel-5P satellite data for air pollution index (API). Third, entropy weight method was applied on indices to generate RSEI and AQRSEI. The RSEI value of KMA is decreased from 0.541 of 2018 to 0.422 of 2021 and further increased from 0.422 of 2021 to 0.534 of 2022. The AQRSEI value of KMA is decreased from 0.547 of 2018 to 0.456 of 2021 and further increased from 0.456 of 2021 to 0.546 of 2022. Both, RSEI and AQRSEI are indirectly related to ecological crisis and KMA shows an upward trend in ecological crisis level within 2018-2022.Thus, effective ecological restoration is needed in KMA.

Keywords Urbanization, spatial technology, eco-environment, air pollution, ecological index.

Introduction

The scientific study of human and environmental interaction and relationship within the zone of interest along with the surrounding elements are known as ecology (Marzluff et al., 2008), (Sutton & Anderson, 2020). The worldwide rapid population growth couple with growing urbanization creates a poor urban ecological health crisis (Newcas, 2021). Several elements which are associated with the urban ecological space are getting disturbed with the continuous unplanned urban growth (Wust et al., 2002). Now a days several eco-environmental problems such as vegetation destruction, water pollution, air pollution, urban heat island etc. are the major issues of concern (De Carvalho & Szlafsztein, 2019), (Ajibade et al., 2020). The identification and analysis of associated factors and elements of urban ecology are becoming crucial in order to deal with such ecological crisis. The monitoring and assessment of ecological condition is not only benefiting human being rather it will help and protect other organisms also (Maity et al., 2022).

The global studies on ecological crisis assessment can be split into two broad categories. The first category focus on ecological impact and risk assessment whereas the second category focus on present ecological condition (Shan et al., 2022). In the traditional approaches of ecological condition study, it involves extensive field-based study and lead to difficulty in data collection and data fusion (H. Xu et al., 2019). To overcome such situation, new way of ecological assessment based on spatial technology are growing importance (Zhu et al., 2020). The spatial technology by means of multidate remote sensing data, GPS, high resolution satellite image has enabled environmentalist to work over any zone of interest with cost-time effectiveness and large-scale monitoring (Firozjaei et al., 2020). Scholars across globe are working extensively on ecological monitoring and eco-environmental assessment based on remotely sensed datasets which is growing popularly as remote sensing based ecological index (RSEI) (Hu & Xu, 2019), (Li et al., 2020), (Wu et al., 2020). The index based ecological assessment needs selection of several suitable indicators which are highly act as affecting factors for ecology.

In context to the ecological condition assessment mainly four indicators such as greenness, dryness, wetness, heat are most affecting factors which needed to be (Cai et al., 2023) and based on it the RSEI model of the Guangxi Beibu Gulf Economic Zone (GBGEZ) during 2001–2020 was assessed (Liao et al., 2022). In very recent, a new approach is growing which urge to add air pollution assessment in ecological index analysis and given the status of air quality based remote sensing ecological index (AQRSEI) (Yue et al., 2019). The RSEI and AQRSEI are highly enabled to quickly detect change in spatial ecological conditions. The availability of high-resolution Landsat 8 Thermal infrared Sensor (TIRS) data for land surface temperature measurement, and Sentinel 2a data for greenness, dryness and wetness analysis coupled with Sentinel 5p satellite data for air quality monitoring made RSEI and AQRSEI measurement more proficient and accurate (Y. Wang et al., 2022). The RSEI and AQRSEI needs indicator weight assignment.

There are several weight assigning models such as analytic hierarchy process (AHP) (Roshani et al., 2023), expert scoring method etc. are available based on subjective judgement which are needed for weight assignment to the indicators of RSEI and AQRSEI. In case of Yangxian, China, AHP–PCA and the minimum cumulative resistance (MCR) model was used to construct an ecological security network based on multi-factor ecological sensitivity (ES) and conduct quantitative spatial analysis (Y. Wang et al., 2022), (Liu et al., 2023). Compare to the subjective based weight assignment model, the object judgement-based Entropy method is most robust one for ecological index analysis based on application (Zongfan et al., 2023). The Entropy was first introduced and used into information theory by Shannon (1997). It is used to assess the degree of dispersion of an indicator. If the degree of dispersion of an indicator is greater then, the weight of that indicator in the evaluation of the composite indicator will be also greater (C. Wang & Zhao, 2019). The basic of the entropy weighting method is to determine weights objectively based on the magnitude of the variability of the indicators; which relies on only the dispersion of the data (J. Wang et al., 2023).

In India, studies have been carried out related to this field on different growing cities such as Delhi (Lu et al., 2019), Mumbai (Rahaman et al., 2021), Kolkata (Das et al., 2021) etc.

but very poor importance were given to air pollution in context of ecological studies. Among Indian metropolitan cities, The Kolkata Metropolitan Area (KMA) of West Bengal is densest and among rapidly growing cities and according to the "The Air Quality and Health in Cities report", 2022 published by the State of Global Air, Kolkata is among the top 20 most polluted cities in the world in terms of PM2.5 levels. Further the increasing pollution and encroachment of an important ecological Ramsar site named east Kolkata wetland (Kumar et al., 2023) coupled with the deteriorating urban ecological health condition of KMA is now becoming a serious issue which need to be studied very crucially. Though of several attempts were made to study KMA ecology, but the crisis in ecological condition of KMA were never studied extensively based on spatial technology, thus there is an immediate need for study regarding ecological crisis of KMA. The main objective of this study to find out ecological crisis of KMA with the help of satellite imagery and develop indicator based two different ecological index and make a comparison between them.

Materials and Methods

Study area: Kolkata Metropolitan Area (KMA) is the outgrowth of the city of Kolkata which is situated at the east bank of river Hooghly. However, the KMA (Figure 1) consists of the twin cities on either side of river Hooghly, viz. Kolkata and Howrah. At present, KMA extends over six districts namely Kolkata, Howrah, Hooghly, Nadia, North 24 Parganas and South 24 Parganas. The area comprises of 4 Municipal Corporation (MC), 37 Municipalities (M) and 23 Panchayat Samities (PS). The approximate geographic extents of the present KMA are about 1876sqkm. According to 2011 census KMA held a population of around 15.87 million as against around 29 million urban population of West Bengal.

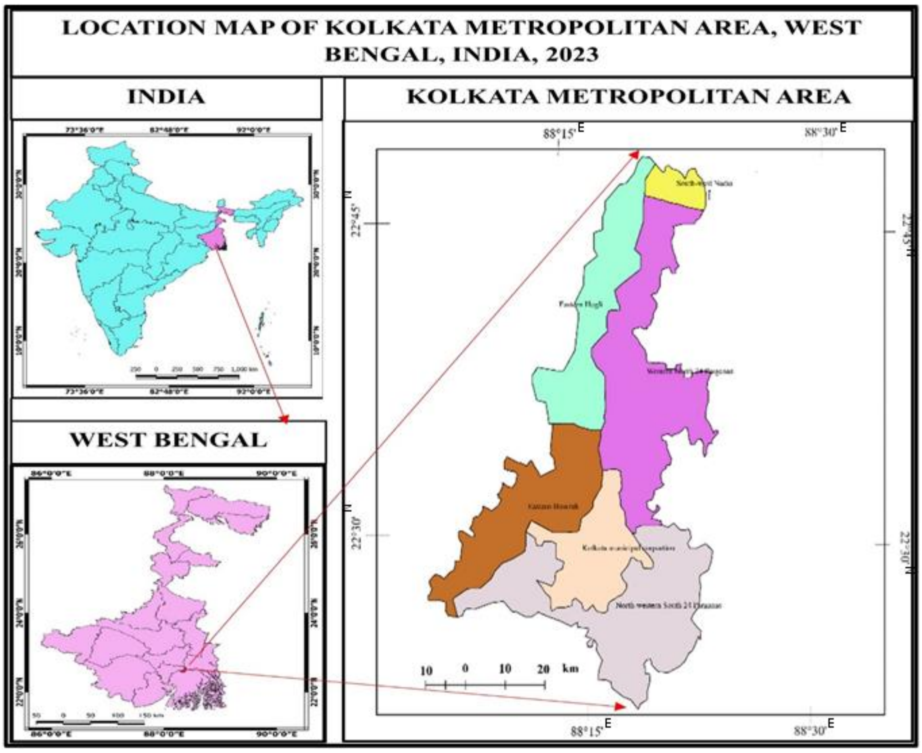

Fig. 1 Location map of Kolkata Metropolitan Area, West Bengal, India, 2023.

Datasets: In this research mainly three different satellite data from 2018 to 2022 were used. First, Landsat 8 thermal infrared sensor (TIRS) with 30 metre resolution data were used to measure land surface temperature (LST) of KMA. Second, Sentinel 2A satellite data with 20 metre resolution were employed to develop Normalized difference vegetation index (NDVI), Modified normalized difference water index (MNDWI) and Normalized difference built up and bare soil index (NDBSI). Third, Sentinel 5P data were used to calculate air pollution index (API).

Methods: In this paper systematic sequential methods were opted. It involves downloading of satellite data followed by preprocessing, indicator generation, weight assignment based on models generated from literature review and thereby final outcome in the form of RSEI and AQRSEI. A methodological flowchart (Figure 2) is shown for clear idea.

Data pre-processing: After downloading the satellite datasets, it was carried out through preprocessing techniques such as atmospheric correction by applying dark object subtraction algorithms (DOS) followed by pan sharpening and radiometric calibrations. Further, images were merged and clipped to extract Kolkata Metropolitan Area (KMA).

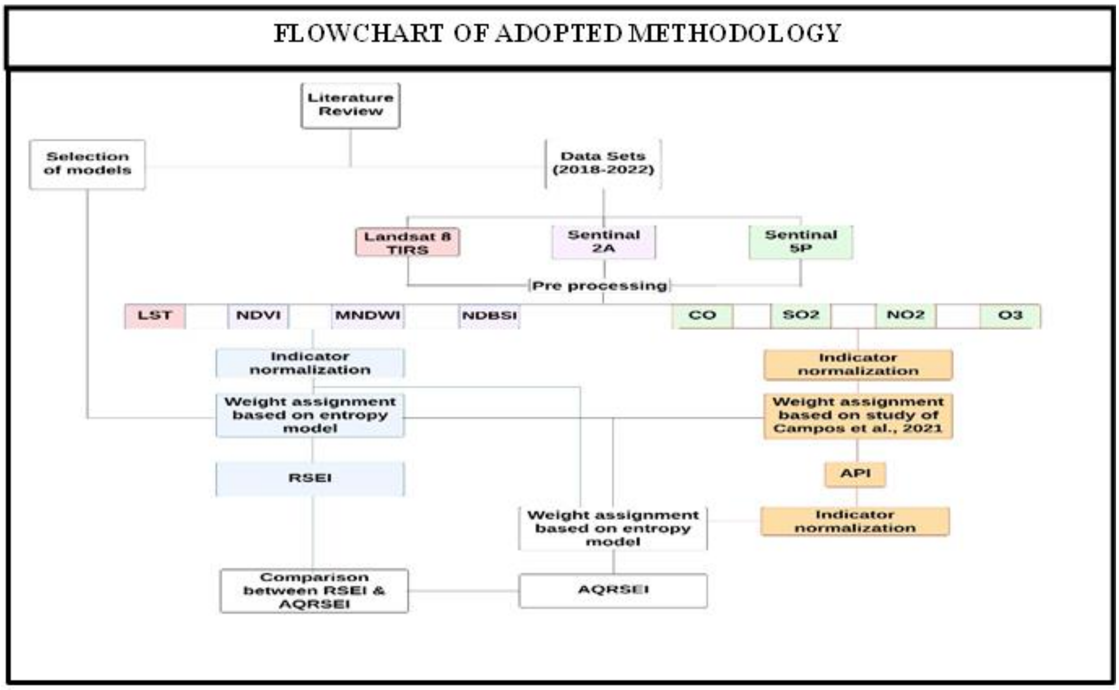

Fig. 2 Flowchart of adopted methodology.

Indices processing: Mainly five indicators were taken into account such as greenness, dryness, wetness, heat and air pollution of the KMA. Different indices were processed by mathematical techniques based on different data source

Greenness index (NDVI): The greenness index of KMA was derived for 2018 to 2022 by representation of the NDVI, which is mainly calculated using satellite remote sensing data to evaluate the growth status of green vegetation in the zone of interest (Huang et al., 2021). The greenness index method is calculated based on the reflection of red and near-infrared light, which can describe productivity, ecosystem vitality, plant growth, and other information (Vélez et al., 2020). It is calculated as:

$$\boldsymbol{NDVI} = (\boldsymbol{NIR} - \boldsymbol{RED})/(\boldsymbol{NIR} + \boldsymbol{RED}) \qquad \text{Eq. (1)}$$

The NIR represents near infrared band whereas RED represents pixel value of red-light reflectance. The value of NDVI ranges in between -1 and +1 where higher value represent high vegetation and vice-versa.

Wetness index (MNDWI): The wetness index of KMA (2018-2022) was mainly represented in the form of MNDWI. The MNDWI mainly identifies open water bodies, reservoirs lakes and rivers (Bie et al., 2020). The MNDWI is calculated based on the reflectance of green and shortwave infrared (SWIR) which is can detect humidity of soil, vegetation and water (Engine, 2020). The calculation of MNDWI is mentioned below:

$$\boldsymbol{MNDWI} = (\boldsymbol{GREEN} - \boldsymbol{SWIR})/(\boldsymbol{GREEN} + \boldsymbol{SWIR}) \qquad \text{Eq. (2)}$$

The value of MNDVI ranges in between -1 and +1 where higher value represent high wetness and vice-versa.

Dryness index (NDBSI): The dryness is expressed by NDBSI which is mainly composed of built-up index (IBI) and bare soil index (SI) which is expressed in follows (X. Wang et al., 2023). In case of IBI calculation, SWIR, near infrared (NIR), green and red band were employed. Further SWIR, red and blue band were used to calculate BI (Yan et al., 2021).

$$\boldsymbol{SI} = ((\boldsymbol{SWIR} + \boldsymbol{RED}) - (\boldsymbol{NIR} + \boldsymbol{BLUE}))/((\boldsymbol{SWIR} + \boldsymbol{RED}) + (\boldsymbol{NIR} + \boldsymbol{BLUE})\ ) \qquad \text{Eq. (3)}$$

$$\boldsymbol{IBI} = (\boldsymbol{2SWIR}/(\boldsymbol{SWIR} + \boldsymbol{NIR}) - (\boldsymbol{NIR}/(\boldsymbol{NIR} + \boldsymbol{RED}) + \boldsymbol{GREEN}/(\boldsymbol{GREEN} + \boldsymbol{SWIR})))/(\boldsymbol{2SWIR}/(\boldsymbol{SWIR} + \boldsymbol{NIR}) + (\boldsymbol{NIR}/(\boldsymbol{NIR} + \boldsymbol{RED}) + \boldsymbol{GREEN}/(\boldsymbol{GREEN} + \boldsymbol{SWIR}))\ ) \qquad \text{Eq. (4)}$$

$$\boldsymbol{NDBSI} = ((\boldsymbol{SI} + \boldsymbol{IBI})/\boldsymbol{2}) \qquad \text{Eq, (5)}$$

The value of NDBSI ranges in between -1 and +1 where higher value represent high dryness and vice-versa. The NDBSI is an important indicator in respect to environment.

Heat (LST): LST is a heat index which is obtained based on single channel algorithm. In this study thermal band 10 of Landsat 8 (TIRS) are used. The LST of KMA was calculated by following sequential steps (Yang et al., 2020). First, the top of atmospheric (TOA) spectral radiance were calculated by following below mention equation:

$$\boldsymbol{L\lambda} = (\boldsymbol{ML}\ \times (\boldsymbol{Qcal}\ +\ \boldsymbol{AL})) \qquad \text{Eq. (6)}$$

Where L_λ represents spectral radiation (Watts / (m^2*sr*um)), M_L represents the Band specific multiplicative rescaling factor from the metadata, (RADIANCE _ MULT _ BAND _ n), Where 'n' represents the band number. (10 for Landsat), Qcal = Level 1 value in DN or Corresponds to band 10 and AL is Band specific additive rescaling factor from the metadata, (RADIANCE _ ADD _ BAND _ n), Where 'n' is the band Number 10. Second, the conversion of TIRS data from spectral radiance to brightness temperature (BTi) occurs according to the below mention equation:

$$\boldsymbol{BTi} = ((\boldsymbol{K2}/\boldsymbol{In}) * (\boldsymbol{K1}/\boldsymbol{L\lambda}) + \boldsymbol{1}) - \boldsymbol{273.15}\ (\boldsymbol{in}\,{}^\circ\,\boldsymbol{C}) \qquad \text{Eq. (7)}$$

where, BTi is top of atmospheric (TOA) brightness temperature in Kelvin or Degree Celsius for TIRS band *i* (Band 10), K1 = Band specific coefficients are thermal conversion constant from the metadata. (K1_CONSTANT_BAND_n), Where 'n' is the band Number 10, K2 = Band specific thermal conversion constant from the metadata. (K2_CONSTANT_BAND_n), Where 'n' is the band Number 10. The result of this process is the temperature in Celsius, and the radiant temperature is the absolute zero temperature is about—273.15OC (Onačillová et al., 2022). Third, NDVI is calculated by using following formula:

$$\boldsymbol{NDVI} = (\boldsymbol{NIR} - \boldsymbol{RED})/(\boldsymbol{NIR} + \boldsymbol{RED}) \qquad \text{Eq. (8)}$$

Where NIR is normal infrared band. Fourth proportion of vegetation (Pv) is calculated by using below mentioned equation:

$$\boldsymbol{Pv} = ((\boldsymbol{NDVI} - \boldsymbol{NDVImin})/(\boldsymbol{NDVImax} - \boldsymbol{NDVImin}))\hat{}\,\mathbf{2} \qquad \text{Eq. (9)}$$

Fifth, land surface emissivity (LSE) is calculated by using below mentioned equation:

$$\in = (\mathbf{0.004} * (\boldsymbol{Pv} + \mathbf{0.986})) \qquad \text{Eq. (10)}$$

Where, ∈ represents LSE. Sixth, final LST is calculated by following equation:

$$\boldsymbol{LST} = (\boldsymbol{BTi}/(\mathbf{1} + (\boldsymbol{\lambda} * \boldsymbol{BT})/\boldsymbol{C2})) * \boldsymbol{In}(\in) \qquad \text{Eq. (11)}$$

where, BT is TOA brightness temperature (°C), λ is Wavelength of emitted radiance (Table - 2), C2 = h*c/s = 14,387.685 μm K; h = Planck's constant = 6.626*10 – 34Js; s = Boltzmann constant = 1.38*10 – 23 J/k; c = Velocity of light = 2.998*10 m/s.

Air Pollution (API): There are several gases which causes pollution in air. In this paper mainly four gases such as nitrogen dioxide (NO2), Carbon monoxide (CO), Ozone (O3), Sulfur dioxide (SO2), are taken into consideration for air pollution index (API) generation (Kaplan & Avdan, 2020). Based upon one study carried by (Campos et al., 2021), the weights are assigned according to degree of harm caused by each pollutant such as NO2 accounts for 70%, SO2 accounts for 15%, O3 accounts for 10%, and CO accounts for 5%. All the four gases are integrated by following below mentioned equation:

$$\boldsymbol{API} = \mathbf{0.7}(\boldsymbol{NO2}) + \mathbf{0.15}(\boldsymbol{SO2}) + \mathbf{0.1}(\boldsymbol{O3}) + \mathbf{0.05}(\boldsymbol{CO}) \qquad \text{Eq. (12)}$$

Remote sensing ecological index (RSEI) & Air quality based remote sensing ecological index (AQRSEI): The RSEI and AQRSEI is an important tool to detect ecological status of an area (Kaplan & Avdan, 2020), (D. Xu et al., 2021). Before calculation of RSEI and AQRSEI, weights are assigned to individual indicators based on entropy model. In order to calculate entropy weight (Z. Wang et al., 2023), the ecological indicators must be discriminated (with forward normalization for the positive indicators of ecology such as NDVI & MNDWI with equation 13 and inverse normalization for the negative indicators of ecology such as NDBSI, LST & API with equation 14) to ensure the reliability of the experimental results using following equations:

$$\boldsymbol{Yij} = (\boldsymbol{Xij} - \mathbf{min}\boldsymbol{Xij})/(\mathbf{max}\boldsymbol{Xij} - \mathbf{min}\boldsymbol{Xij}) \qquad \text{Eq. (13)}$$

$$\boldsymbol{Yij} = (\boldsymbol{maxXij} - \boldsymbol{Xij})/(\mathbf{max}\boldsymbol{Xij} - \mathbf{min}\boldsymbol{Xij}) \qquad \text{Eq. (14)}$$

Where, Yij represents the normalized value, Xij represents the original value of each indicator, minXij represents the minimum value of each indicator, and maxXij represents the maximum value of each indicator. Further, weight is assigned to four indicators such as NDVI, MNDWI, NDBSI and LST based on entropy model And RSEI is calculated using following equation:

$$\boldsymbol{RSEI} = ((\mathbf{0.2509} * \boldsymbol{NDVI}) + (\mathbf{0.2504} * \boldsymbol{MNDWI}) + \mathbf{0.2486} * \boldsymbol{NDBSI}) + (\mathbf{0.2499} * \boldsymbol{LST})) \quad \text{Eq. (15)}$$

After RSEI calculation, again weight is assigned based upon entropy calculation to five indicators such as NDVI, MNDWI, NDBSI, LST and API and AQRSEI is derived by following below mentioned equation:

$$\boldsymbol{AQRSEI} = ((\mathbf{0.2006} * \boldsymbol{NDVI}) + (\mathbf{0.2002} * \boldsymbol{MNDWI}) + \mathbf{0.1987} * \boldsymbol{NDBSI}) + (\mathbf{0.1998} * \boldsymbol{LST}) + (\mathbf{0.2004} * \boldsymbol{API})) \quad \text{Eq. (16)}$$

Here the value of RSEI and AQRSEI are ranges in between 0 to 1 where lower value represent high ecological crisis and higher value represent lower ecological crisis. To accomplish all the software related work, Q-GIS 3.16 version and ARC GIS 10.9 version were used.

Results and discussions

Indicators: Primarily four indicators such as NDVI, MNDWI, NDBSI and LST are taken into account for calculation and generation of RSEI map of the study area. In case of AQRSEI calculation and map development of study area, total five indicators are taken into account named NDVI, MNDWI, NDBSI, LST and API. These indicators are taken into consideration to see its impact upon the ecological status by means of RSEI and AQRSEI. Thereby detailed analysis of indicators is discussed below.

Greeness: NDVI which is an important positive indicator for RSEI and AQRSEI. Generally, NDVI measures greenness of an area. It is an important parameter for vegetation monitoring, agriculture, land use planning, environmental studies and monitoring ecological status. It gives objective and quantitative information of greenness of an area. The value of NDVI of KMA is ranges in between 0 to 1 because it is shown here after normalization. Higher value represents high vegetation and vice-versa. The mean NDVI value of KMA (Table 1) is changing within five years where the value is increased from 0.649 of 2018 to 0.663 of 2020 and then decreased from 0.663 of 2020 to 0.528 of 2022. If we compare mean NDVI value within particularly 2018 and 2022 year, then the mean NDVI is showing a decreasing trend from 0.649 to 0.528. Thus, a downfall in vegetation can be seen within the five-year span of time in KMA but remarkably within 2020 to 2022. The map (Figure 3) showing a remarkable change from 2018 to 2022 in central part of KMA towards low NDVI.

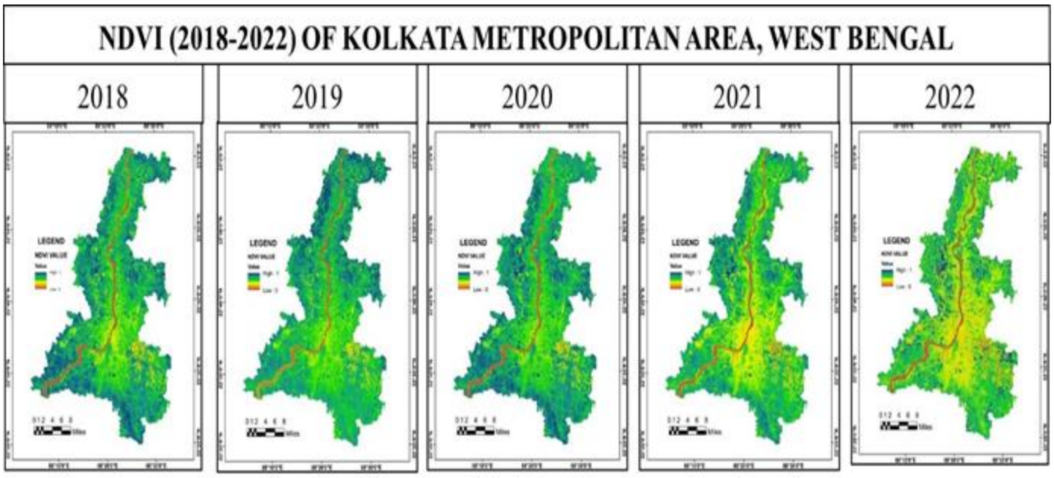

Fig. 11. NDVI (2018-2022) of KMA.

Table 1 Year wise (2018-2022) change in NDVI, MNDWI, NDBSI, LST, API, RSEI and AQRSEI of KMA.

YEAR	NDVI	MNDWI	NDBSI	LST	API	RSEI	AQRSEI
2018	0.3252	0.1347	0.2132	20.7995	0.4303	0.5420	0.5472
2019	0.3401	0.2017	0.1834	29.1933	0.2172	0.4773	0.5304
2020	0.3344	0.1870	0.1805	21.5200	0.2293	0.4336	0.4922
2021	0.2845	0.1630	0.1869	23.7341	0.3950	0.4229	0.4567
2022	0.2725	0.2080	0.0618	20.5067	0.3970	0.5341	0.5463

Wetness: In case of good ecological measurement wetness is an important element. To detect and measure wetness of KMA, MNDWI is calculated. The MNDWI is useful in applications involving flood mapping, resource management and environmental monitoring. The value of MNDWI of KMA is ranges in between 0 to 1 because it is shown here after normalization. MNDWI is a positive indicator of RSEI and AQRSEI.

The average MNDWI of KMA (Table 1) is decreased from 0.363 of 2018 to 0.262 of 2019 and further, increased from 0.262 of 2019 to 0.391 of 2022. In case whole five years the mean MNDWI got increased from 0.363 of 2018 to 0.391 of 2022. The overall MNDWI map (Figure 4) showing more waterbody concentration toward south east KMA and some patches toward northern portion. The presence of high MNDWI value is highly suitable for high RSEI and AQRSEI.

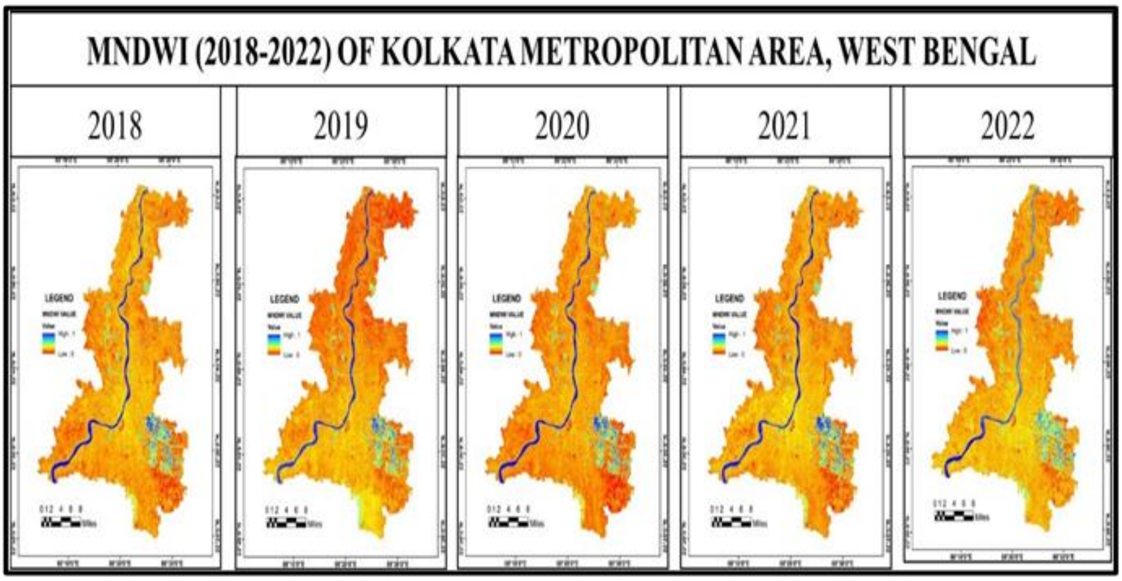

Fig. 12 MNDWI (2018-2022) of KMA.

Dryness: The soil and built-up area are an important factor of ecology. By putting soil and built-up together NDBSI is calculated to determine dryness of KMA. The NDBSI represent dryness of an area which is highly useful in several studies which involves soil classification, urban planning, agriculture, eco-environment monitoring etc. The value of NDBSI of KMA is ranges in between 0 to 1 because it is shown here after normalization. The NDBSI is negative indicators of RSEI and AQRSEI.

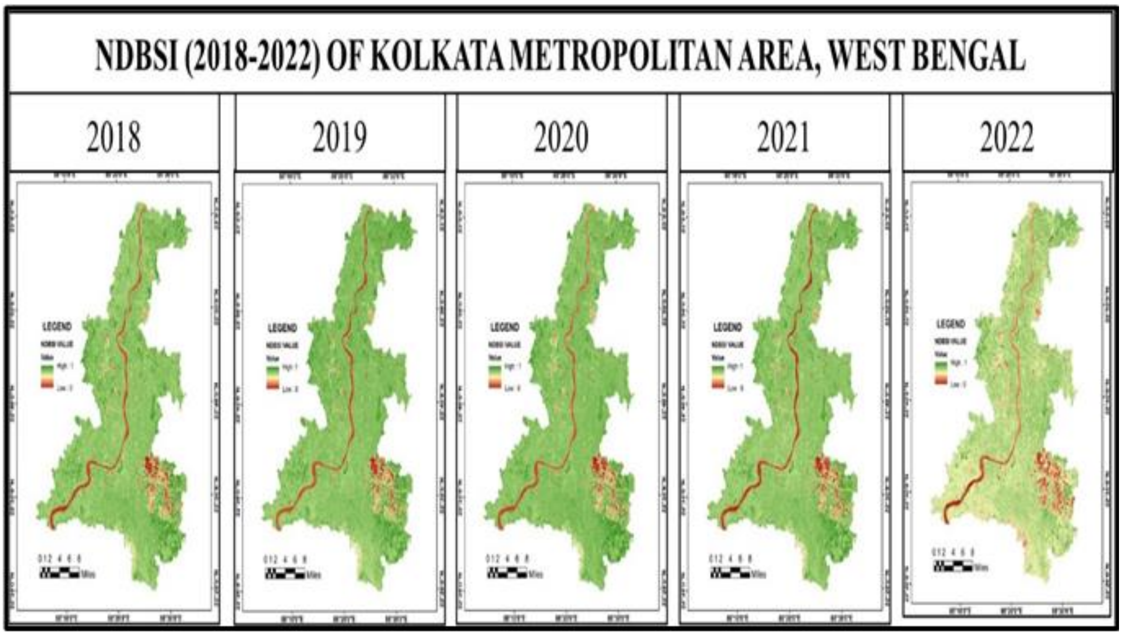

Fig. 13 NDBSI (2018-2022) of KMA.

The mean NDBSI value of KMA (Table 1) is decreased from 0.458 of 2018 to 0.309 of 2020 but increased from 0.309 of 2020 to 0.615 of 2022. The overall NDBSI map (Figure 5) of all year are showing low dryness toward south east Kolkata and throughout the waterbody portions where high dryness toward central KMA or built-up region. Particularly within five years span mean NDBSI or dryness increases from 0.458 of 2018 to 0.615 of 2022.

Heat: The ecological condition of an area is highly affected by surface temperature. The LST is an important indicator of RSEI and AQRSEI, which represents heat of an area. The value of LST of KMA is ranges in between 0 to 1 because it is shown here after normalization. The LST is mainly influenced by surface properties, atmospheric conditions, thermal properties of an area and affect negatively to RSEI and AQRSEI.

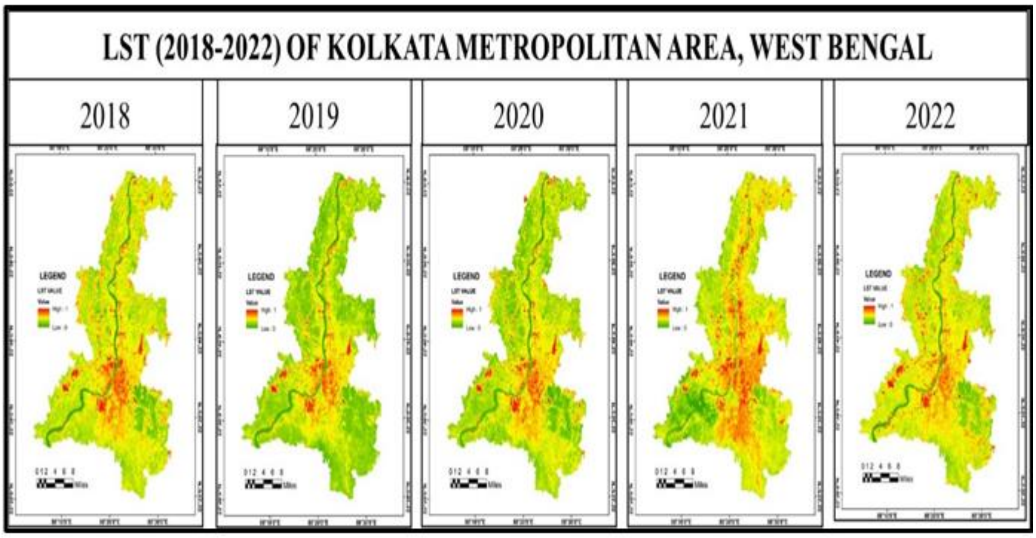

Fig. 14 LST (2018-2022) of KMA.

The average LST value of KMA (Table 6) is decreased from 0.696 of 2018 to 0.426 of 2021 and further increased from 0.426 of 2021 to 0.603 of 2022. If we compare mean LST value within particularly 2018 and 2022 year, then the mean LST is showing a decreasing trend from 0.696to 0.603. The LST of all map (Figure 6) showing higher value and increasing trend in central part compared to other of KMA.

Air Quality: The air quality of KMA is measured by means of API which is negative indicator of RSEI and AQRSEI. The concentration of CO, NO2, O3 and SO2 gas are taken into consideration to calculate API of KMA. The API of KMA is ranges in between 0 to 1 because it is shown here after normalization. The API is highly useful in the study of climate change, environmental protection and urban planning etc.

The API mean value of KMA (Table 1) is increased from 0.568 of 2018 to 0.726 of 2020 but decreased from 0.726 of 2020 to 0.594 of 2021 and further increased a little bit from 0.594 of 2021 to 0.595 of 2023. Overall, the API of KMA (Figure 7) is highly concentrated in the southern KMA but moves toward western KMA in 2022.

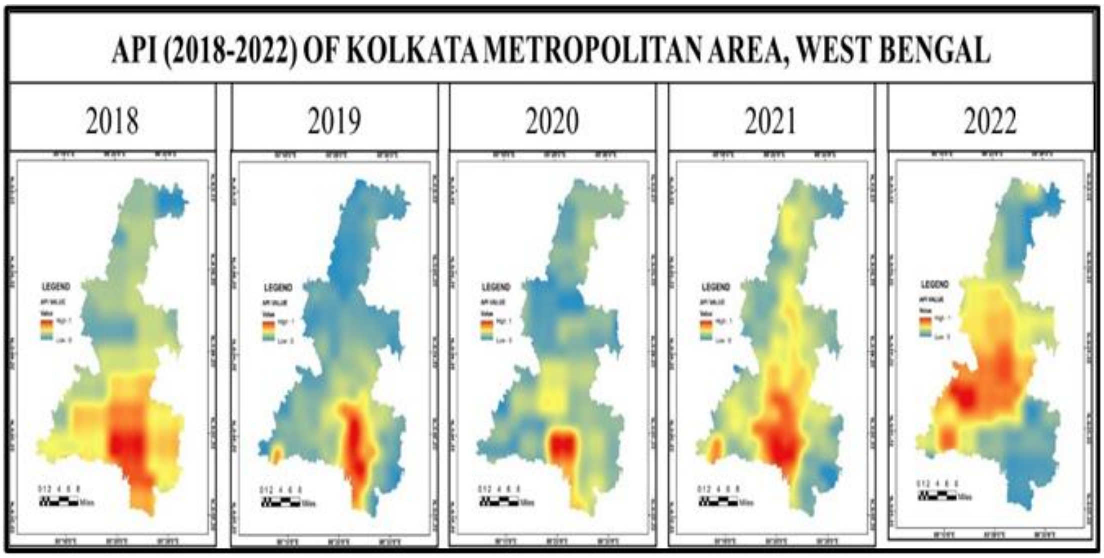

Fig. 7 API (2018-2022) of KMA.

Ecological crisis of KMA: The ecological crisis of an area can be well understood by the help of RSEI and AQRSEI. If there is higher RSEI and AQRSEI value then it represents a low crisis in ecological health and vice-versa.

Remote sensing ecological index (RSEI): The RSEI is a satellite image-based tool and metrics used to measure various ecological parameter of zone of interest and mainly detect ecological status of an area. The RSEI of KMA is calculated based on four important indicators namely NDVI, MNDWI, NDBSI and LST from 2018 to 2022. The RSEI value of KMA is ranges in between 0 to 1 as it is shown here after normalization.

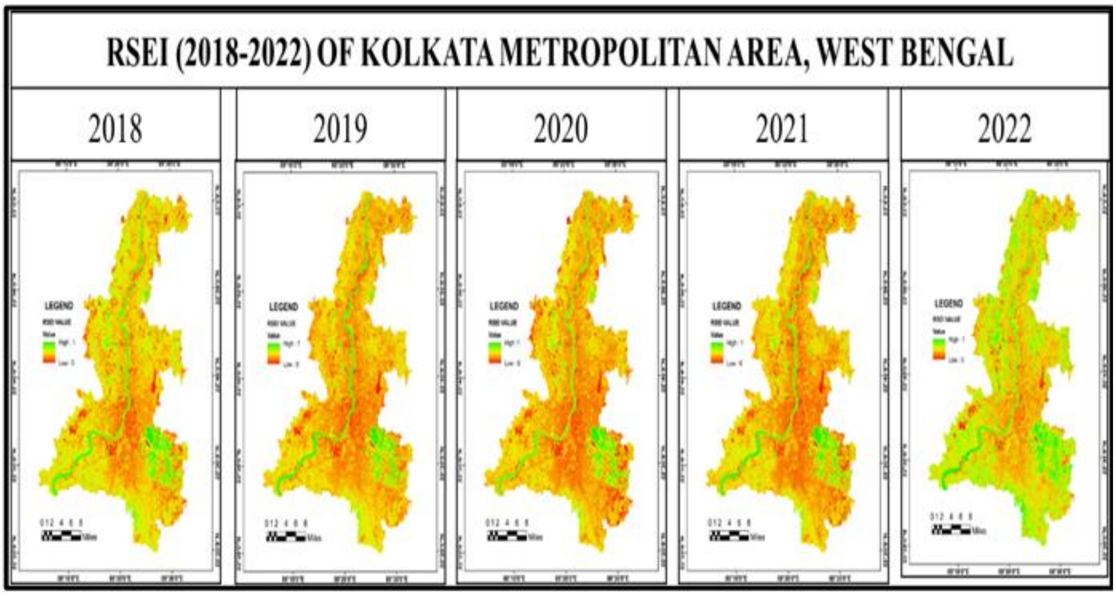

Fig. 8 RSEI (2018-2022) of KMA.

The RSEI value of KMA (Table 1) is decreased from 0.541 of 2018 to 0.422 of 2021 and further increased from 0.422 of 2021 to 0.534 of 2022. In case of all the map (Figure 8) a high RSEI can be observed in case of south east and western KMA whereas a low RSEI in case of central part of KMA. If we compare RSEI of particularly 2018 and 2022 then we can observe a declining from 0.541 of 2018 to 0.534 of 2022.

Air quality based remote sensing ecological index (AQRSEI): The AQRSEI is mainly used to see the impact ecological impact of air pollution over the study area. Based on five important indicators such as NDVI, MNDWI, NDBSI, LST and API, the AQRSEI is calculated for KMA. The AQRSEI value of KMA is ranges in between 0 to 1 as it is shown here after normalization. The AQRSEI play vital role in monitoring and assessing the effects of air pollution on ecosystem.

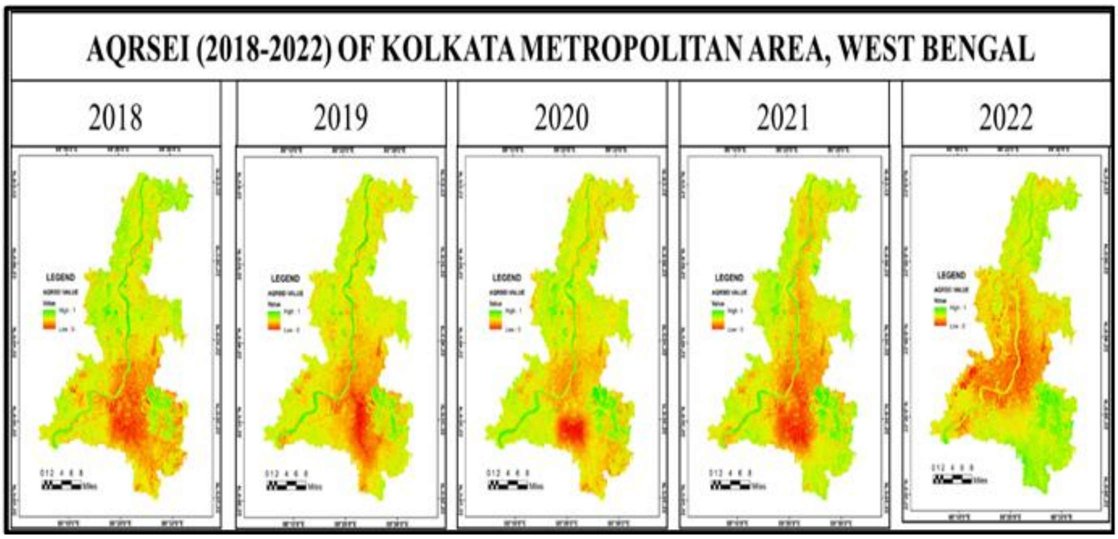

Fig. 15 AQRSEI (2018-2022) of KMA.

The AQRSEI value of KMA (Table 1) is decreased from 0.547 of 2018 to 0.456 of 2021 and further increased from 0.456 of 2021 to 0.546 of 2022. If we compare RSEI of particularly 2018 and 2022 then we can observe a declining from 0.547 of 2018 to 0.546 of 2022. In case of all the map (Figure 9) a high AQRSEI can be observed in case of south east and western KMA whereas a low RSEI in case of central part of KMA.

Comparison between RSEI and AQRSEI: The comparison between RSEI and AQRSEI of KMA (Figure 10) is showing a change in year wise index value. In case of each year from 2018 to 2022 the AQRSEI value is comparatively higher then RSEI value of KMA. It means the AQRSEI is representing low ecological crisis compared to RSEI.

The RSEI and AQRSEI value of KMA (Table 1), both are decreased from 2018 to 2021 which indicates high ecological crisis within this year but further the value is increased in 2022 which represent a recovery in crisis. If we compare RSEI and AQRSEI of particularly 2018 and 2022 then we can observe a declining from 2018 to 2022. The trend line (Figure 10) in case of RSEI and AQRSEI are showing negative trend which expect an increase in ecological crisis in near future. Both the RSEI and AQRSEI showing low value, where there is built-up zone in KMA whereas they showing higher value where there is vegetation, wetlands, agricultural land etc.

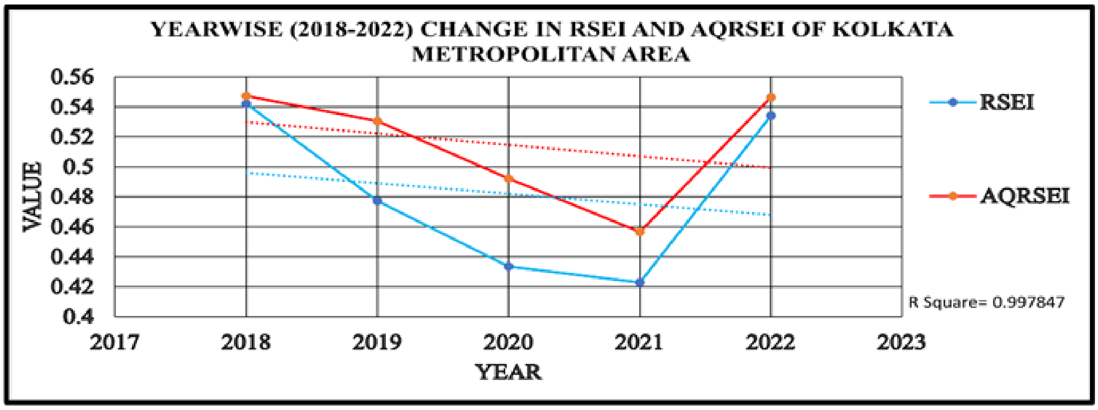

Fig. 16 Year wise (2018-2022) change in RSEI and AQRSEI of KMA.

Conclusions

The KMA which is an important city whose ecological crisis assessment is very much crucial as it is in thereat of rapid population growth, unplanned urbanization and air pollution. The ecological crisis of KMA within a time span of five years from 2018 to 2022 are being done by means of RSEI and AQRSEI. The RSEI and AQRSEI shows a decrease in value particularly within 2018 and 2022 year. The downfall in RSEI and AQRSEI value creates a form of ecological crisis which is increasing. Further, trend line of both RSEI and AQRSEI is negative which represent a high ecological crisis in near future. The AQRSEI is better as it is taking more indicators in consideration in comparison to RSEI. It is to be mentioned that both RSEI and AQRSEI have indirect relationship with ecological crisis. In order to deal with the ecological crisis several strategies have to be adopted in case of KMA such as afforestation, water conservation, reduction, recycling and pollution control, support sustainable agriculture, environmental legislation and regulation, transit to clean energy etc.

Acknowledgements

The authors great fully thanks to department of geography, Central University of Punjab for their laboratory facilities and kind encouragement.

References

Ajibade, F. O., Adelodun, B., Lasisi, K. H., Fadare, O. O., Ajibade, T. F., Nwogwu, N. A., Sulaymon, I. D., Ugya, A. Y., Wang, H. C., & Wang, A. (2020). Environmental pollution and their socioeconomic impacts. In *Microbe Mediated Remediation of Environmental Contaminants* (Issue November).

Bie, W., Fei, T., Liu, X., Liu, H., & Wu, G. (2020). Small water bodies mapped from Sentinel-2 MSI (MultiSpectral Imager) imagery with higher accuracy. *International Journal of Remote Sensing*, *41*(20), 7912–7930.

Cai, Z., Zhang, Z., Zhao, F., Guo, X., Zhao, J., Xu, Y., & Liu, X. (2023). Assessment of eco-environmental quality changes and spatial heterogeneity in the Yellow River Delta based on the remote sensing ecological index and geo-detector model. *Ecological Informatics*, *77*(July), 102203.

Campos, P. M. D., Esteves, A. F., Leitão, A. A., & Pires, J. C. M. (2021). Design of air quality monitoring network of Luanda, Angola: Urban air pollution assessment. *Atmospheric Pollution Research*, *12*(8).

Das, M., Das, A., Pereira, P., & Mandal, A. (2021). Mapping the impact of COVID-19 lockdown on urban surface ecological status (USES): A case study of Kolkata Metropolitan Area (KMA), India. *Remote Sensing*, *13*(21).

De Carvalho, R. M., & Szlafsztein, C. F. (2019). Urban vegetation loss and ecosystem services: The influence on climate regulation and noise and air pollution. *Environmental Pollution*, *245*, 844–852.

Engine, E. (2020). *Sentinel-1-Imagery-Based High-Resolution Water Cover Detection on Wetlands , Aided by Google Earth Engine*. 1–20.

Firozjaei, M. K., Fathololoumi, S., Weng, Q., Kiavarz, M., & Alavipanah, S. K. (2020). Remotely sensed urban surface ecological index (RSUSEI): An analytical framework for assessing the surface ecological status in urban environments. *Remote Sensing*, *12*(12).

Hu, X., & Xu, H. (2019). A new remote sensing index based on the pressure-state-response framework to assess

regional ecological change. *Environmental Science and Pollution Research*, *26*(6), 5381–5393.
Huang, S., Tang, L., Hupy, J. P., Wang, Y., & Shao, G. (2021). A commentary review on the use of normalized difference vegetation index (NDVI) in the era of popular remote sensing. *Journal of Forestry Research*, *32*(1), 1–6.
Kaplan, G., & Avdan, Z. Y. (2020). Space-Borne Air Pollution Observation From Sentinel-5P Tropomi: Relationship Between Pollutants, Geographical and Demographic Data. *International Journal of Engineering and Geosciences*, *5*(3), 130–137.
Kumar, N., Chandan, N. K., Bhushan, S., Singh, D. K., & Kumar, S. (2023). Health risk assessment and metal contamination in fish , water and soil sediments in the East Kolkata Wetlands , India , Ramsar site. *Scientific Reports*, 1–18.
Li, J., Pei, Y., Zhao, S., Xiao, R., Sang, X., & Zhang, C. (2020). A review of remote sensing for environmental monitoring in China. *Remote Sensing*, *12*(7), 1–25.
Liao, W., Jiang, W., & Huang, Z. (2022). Spatiotemporal variations of eco-environment in the Guangxi Beibu Gulf Economic Zone based on remote sensing ecological index and granular computing. *Journal of Geographical Sciences*, *32*(9), 1813–1830.
Liu, L., Chen, M., Luo, P., Duan, W., & Hu, M. (2023). Quantitative Model Construction for Sustainable Security Patterns in Social–Ecological Links Using Remote Sensing and Machine Learning. *Remote Sensing*, *15*(15). https://doi.org/10.3390/rs15153837
Lu, L., Weng, Q., Guo, H., Feng, S., & Li, Q. (2019). Assessment of urban environmental change using multi-source remote sensing time series (2000–2016): A comparative analysis in selected megacities in Eurasia. *Science of the Total Environment*, *684*, 567–577.
Maity, S., Das, S., Pattanayak, J. M., Bera, B., & Shit, P. K. (2022). Assessment of ecological environment quality in Kolkata urban agglomeration, India. *Urban Ecosystems*, *25*(4), 1137–1154.
Marzluff, J. M., Endlicher, W., Bradley, G., Simon, U., Shulenberger, E., Alberti, M., Ryan, C., & Zumbrunnen, C. (2008). Urban ecology: An international perspective on the interaction between humans and nature. *Urban Ecology: An International Perspective on the Interaction Between Humans and Nature*, *January 2008*, 1–807.
Newcas, J. (2021). *’ Population and our contemporary ecological crisis ’. in C . Nellist , ed . Climate Crisis and Creation Care : Historical Perspectives , Ecological Integrity*.
Onačillová, K., Gallay, M., Paluba, D., Péliová, A., Tokarčík, O., & Laubertová, D. (2022). Combining Landsat 8 and Sentinel-2 Data in Google Earth Engine to Derive Higher Resolution Land Surface Temperature Maps in Urban Environment. *Remote Sensing*, *14*(16).
Rahaman, S., Jahangir, S., Haque, M. S., Chen, R., & Kumar, P. (2021). Spatio-temporal changes of green spaces and their impact on urban environment of Mumbai, India. *Environment, Development and Sustainability*, *23*(4), 6481–6501.
Roshani, Sajjad, H., Rahaman, M. H., Rehman, S., Masroor, M., & Ahmed, R. (2023). Assessing forest health using remote sensing-based indicators and fuzzy analytic hierarchy process in Valmiki Tiger Reserve, India. *International Journal of Environmental Science and Technology*, *20*(8), 8579–8598.
Shan, Y., Dai, X., Li, W., Yang, Z., Wang, Y., Qu, G., Liu, W., Ren, J., Li, C., Liang, S., & Zeng, B. (2022). Detecting Spatial-Temporal Changes of Urban Environment Quality by Remote Sensing-Based Ecological Indices: A Case Study in Panzhihua City, Sichuan Province, China. *Remote Sensing*, *14*(17), 1–25.
Sutton, M. Q., & Anderson, E. N. (2020). Fundamentals of Ecology. *Introduction to Cultural Ecology*, 31–52.
Vélez, S., Barajas, E., Rubio, J. A., Vacas, R., & Poblete-Echeverría, C. (2020). Effect of missing vines on total leaf area determined by NDVI calculated from sentinel satellite data: Progressive vine removal experiments. *Applied Sciences (Switzerland)*, *10*(10).
Wang, C., & Zhao, H. (2019). Analysis of remote sensing time-series data to foster ecosystem sustainability: use of temporal information entropy. *International Journal of Remote Sensing*, *40*(8), 2880–2894.
Wang, J., Zhang, F., Tan, M. L., Shi, J., Johnson, V. C., & Kung, H. Te. (2023). Remote sensing evaluation of Chinese mainland’s comprehensive natural resources carrying capacity and its spatial-temporal variation characteristics. *Environmental Impact Assessment Review*, *101*(March), 107104. https://doi.org/10.1016/j.eiar.2023.107104
Wang, X., Zhang, S., Zhao, X., & Shi, S. (2023). *Exploring the Relationship between the Eco-Environmental Quality and Urbanization by Utilizing Sentinel and Landsat Data : A Case Study of the Yellow River Basin*.
Wang, Y., Cai, G., Yang, L., Zhang, N., & Du, M. (2022). Monitoring of urban ecological environment including air quality using satellite imagery. *PLoS ONE*, *17*(8 August), 1–15.
Wang, Z., Chen, T., Zhu, D., Jia, K., & Plaza, A. (2023). RSEIFE: A new remote sensing ecological index for simulating the land surface eco-environment. *Journal of Environmental Management*, *326*(PA), 116851. https://doi.org/10.1016/j.jenvman.2022.116851
Wu, J., Wang, X., Zhong, B., Yang, A., Jue, K., Wu, J., Zhang, L., Xu, W., Wu, S., Zhang, N., & Liu, Q. (2020). Ecological environment assessment for Greater Mekong Subregion based on Pressure-State-Response framework by remote sensing. *Ecological Indicators*, *117*(September 2019), 106521. https://doi.org/10.1016/j.ecolind.2020.106521
Wust, S., Bolay, J. C., & Ngoc Du, T. T. (2002). Metropolization and the ecological crisis: Precarious settlements in

Ho Chi Minh City, Vietnam. *Environment and Urbanization*, *14*(2), 211–224.

Xu, D., Yang, F., Yu, L., Zhou, Y., Li, H., Ma, J., & Huang, J. (2021). *Quantization of the coupling mechanism between eco-environmental quality and urbanization from multisource remote sensing data*. *321*.

Xu, H., Wang, Y., Guan, H., Shi, T., & Hu, X. (2019). Detecting ecological changes with a remote sensing based ecological index (RSEI) produced time series and change vector analysis. *Remote Sensing*, *11*(20), 1–24.

Yan, Y., Yu, X., Long, F., & Dong, Y. (2021). A multi-criteria evaluation of the urban ecological environment in shanghai based on remote sensing. *ISPRS International Journal of Geo-Information*, *10*(10).

Yang, J., Zhou, J., Göttsche, F. M., Long, Z., Ma, J., & Luo, R. (2020). Investigation and validation of algorithms for estimating land surface temperature from Sentinel-3 SLSTR data. *International Journal of Applied Earth Observation and Geoinformation*, *91*(April), 102136.

Yue, H., Liu, Y., Li, Y., & Lu, Y. (2019). Eco-environmental quality assessment in china's 35 major cities based on remote sensing ecological index. *IEEE Access*, *7*, 51295–51311.

Zhu, D., Chen, T., Zhen, N., & Niu, R. (2020). Monitoring the effects of open-pit mining on the eco-environment using a moving window-based remote sensing ecological index. *Environmental Science and Pollution Research*, *27*(13), 15716–15728.

Zongfan, B., Ling, H., Huiqun, L., Xuhai, J., & Liangzhi, L. (2023). Spatiotemporal change and driving factors of ecological status in Inner Mongolia based on the modified remote sensing ecological index. *Environmental Science and Pollution Research*, *30*(18), 52593–52608.

Citation

Mitra, P. Mustak, S.K., Barman, P. (2024). Monitoring Ecological Crisis of Kolkata Metropolitan Area using Spatial Technology. In: Dandabathula, G., Bera, A.K., Rao, S.S., Srivastav, S.K. (Eds.), Proceedings of the 43rd INCA International Conference, Jodhpur, 06–08 November 2023, pp. 532–546, ISBN 978-93-341-2277-0.